RESEARCH ARTICLE

Evaluation of Quantitative Imaging Biomarkers in the DSS Colitis Model

Anne Beltzer,[1] Thomas Kaulisch,[1] Teresa Bluhmki,[1] Tanja Schoenberger,[2] Birgit Stierstorfer,[2] Detlef Stiller[1]

[1]Div. Research Germany–Target Discovery Research, In-Vivo Imaging Laboratory, Boehringer Ingelheim Pharma GmbH & Co. KG, Birkendorfer Straße 65, 88397, Biberach an der Riß, Germany
[2]Target Discovery Research, Target Validation Technologies, Boehringer Ingelheim Pharma GmbH & Co. KG, Biberach an der Riss, Germany

Abstract

Purpose: In humans, colonoscopy is the gold standard for the diagnosis of inflammatory changes of the colon wall. Aim of this study was the identification of less invasive imaging biomarkers in the dextran sodium sulfate (DSS) colitis model to provide additional information on transmural changes of the colon wall.
Procedures: Colitis was induced in C57BL/6 mice by administration of 2, 3, and 4 % DSS over a period of 5 days. Colon wall thickness was measured using magnetic resonance imaging (MRI), ultrasound (US), and x-ray computed tomography (CT), gut inflammation by positron emission tomography/CT, and mucosal changes of the colon wall by colonoscopy. Colon samples were examined histologically.
Results: MRI, CT, US, and histological data revealed increased colon wall thickness in DSS-treated mice compared to healthy controls. Elevated 2-deoxy-2-[^{18}F]fluoro-D-glucose uptake and colonoscopy confirmed high inflammatory load in the guts of colitis mice.
Conclusions: The established quantitative imaging readouts offer promising perspectives to develop new compounds and to translate these methods into the clinical setting.

Key words: DSS, Mouse model, Colitis, Inflammatory bowel disease, Multimodal imaging

Abbreviations: CT, Computed tomography; MRI, Magnetic resonance imaging; PET/CT, Positron emission tomography combined with computed tomography; US, Ultrasound imaging; SPECT, Single photon emission computed tomography; [^{18}F]FDG, 2-deoxy-2-[^{18}F]fluoro-D-glucose; DSS, Dextran sodium sulfate; IBD, Inflammatory bowel disease

Introduction

Inflammatory bowel disease (IBD) is a chronic inflammatory disorder of the gastrointestinal tract comprising the two main prototypes Crohn's disease and ulcerative colitis [1]. Patients with IBD can suffer from diarrhea, rectal bleeding, and abdominal pain, and exhibit clinical signs of bowel destruction and formation of strictures, fistulas, or abscesses [2]. As the pathogenesis of IBD remains largely unclear and therapy options are limited, most of the patients in a progressive state of illness rely on hospitalization and surgical intervention which may result in a loss of quality of life.

Ileocolonoscopy is the gold standard technique for diagnosis of IBD [3, 4]. This examination allows direct inspection of structural inflammatory and neoplastic changes of the mucosal surface of IBD patients as well as the removal of tissue samples for pathological analysis.

However, a drawback of colonoscopy is the restriction to the mucosal surface without the option to detect extracolonic lesions.

Whereas endoscopy is a well-established diagnostic procedure in the clinical routine, the other non-invasive imaging techniques such as magnetic resonance imaging (MRI), ultrasound (US), x-ray computed tomography (CT), or positron emission tomography combined with x-ray computed tomography (PET/CT) are not used as standard procedures for assessment of IBD [5–7]. Less invasive imaging techniques than colonoscopy would be desirable to longitudinally follow-up course of disease and treatment success. MRI, US, and CT may provide useful information on colon wall thickness as a measure of inflammatory burden, for detection of transmural and extraluminal complications and to monitor disease progression. PET/CT using 2-deoxy-2-[^{18}F]fluoro-D-glucose ([^{18}F]FDG) has also been shown to provide information on inflammatory activity of IBD patients [8, 9]. Both PET and SPECT can also be used for specific cell tracking, e.g., macrophages or neutrophils [10].

A commonly used preclinical model to study IBD is the dextran sodium sulfate (DSS) colitis model that shows several characteristics of the human disease such as rectal bleedings and diarrhea [11, 12]. Several imaging techniques have been applied in the DSS model, but to our knowledge, none of these studies have shown a direct comparison of different imaging methods in this model.

In this study, we compared non-invasive imaging techniques (MRI, US, CT, and PET/CT) to endoscopy in the DSS colitis model, and estimated the severity of inflammatory lesions by establishing quantitative imaging readouts which need to be further evaluated for their potential in a therapeutic setting of this model.

Materials and Methods

Animals and DSS Colitis

Animal experiments were approved by the animal care committee of the regional board Tübingen and were conducted in accordance with the regulations of the German Federal Law on Care and Use of Laboratory Animals.

Eight- and 11-week-old female C57BL/6 (C57BL/6NCrl) mice were purchased from Charles River Laboratories (Sulzfeld, Germany). For colitis induction, 2, 3, or 4 % DSS (MP Biomedicals, Germany) were added to the drinking water of mice for 5 days. Animal body weights and disease activity (disease activity index (DAI) as described in [13]: body weight loss (1 point for each 5 % loss of weight), stool consistency (0, normal; 2, formed but very soft; 4, liquid), presence of gross blood in the stools (macroscopically) (0, none; 1, present)) were monitored regularly until the end of the experiment at day 9. Two separate studies were performed to assess mucosal changes by colonoscopy, colon wall thickness by MRI, US, and CT and inflammatory lesions by [^{18}F]FDG PET/CT.

In the first experiment, DSS colitis was induced in 11-week-old mice: MRI, US, and colonoscopy were performed at day 8, except for the control and 2 % DSS group in which colonoscopy was performed at day 9. Animals were euthanized at day 8 (3 and 4 % DSS) or at day 9 (control group and 2 % DSS). The colons were removed to measure colon length and were collected for histological examination.

In the second experiment, DSS colitis was induced in 8-week-old mice: In addition to colonoscopy, MRI and US (data not shown) animals were assessed by CT and PET/CT at day 7. At euthanization, whole blood was collected via the facial vein and the colons were removed to measure colon length and for histological examination (data not shown).

The methods used for imaging and histologic analyses are detailed below.

Colonoscopy for Endoscopic Colitis Score

For murine endoscopy, the Coloview miniendoscopic system (Karl Storz, Tuttlingen, Germany) was used according to the protocol of Becker et al. [14]. The scope was lubricated with water and carefully inserted into the anus of the mouse anesthetized with 1.5–2 % isoflurane. Under insufflation with air, the scope was advanced up to the splenic flexure. During withdrawal of the scope, videos were captured to examine the mucosa and perform the scoring subsequently offline. Colitis severity was determined evaluating the thickening of the colon wall, the vascular pattern, the presence of fibrin, the granularity of the mucosal surface, and the stool consistency (murine endoscopic index of colitis severity, see Becker et al. [14]). The scorer was blinded to the treatment groups.

MRI for Colon Wall Thickness

Animals were anesthetized with 1.5–2 % isoflurane, rectally inserted with a soft hollow tube and placed in a supine position on the animal bed of a 7T small animal scanner (Pharmascan, Bruker BioSpin, Ettlingen, Germany). For image acquisition, a RARE sequence was used to generate axial images of the colon (TR = 3000 ms, TE = 36 ms, slice thickness 1 mm, field of view 2.56×2.56 cm^2, matrix 256×256, 4 averages, scan time 6 min 24 s).

For image analysis, three colon wall thickness measurements were performed in an axial position approximately 1.5 cm from the anus using ParaVision 5.1 software. Colon wall thickness was defined as the average of the data.

US for Colon Wall Thickness

Transabdominal ultrasound was performed by the Vevo 2100 high-resolution imaging system (Visual Sonics, Amsterdam, Netherlands) in B-mode (brightness) and M-mode (motion) using the MS-550D transducer (center frequency 40 MHz). Mice were anesthetized with 1.5–2 % isoflurane and were positioned in the supine position. Ultrasound gel was injected into the rectum before intestinal images approximately 1.5 cm from the anus were acquired. Three colon wall thickness measurements were made in M-mode images using Vevo 2100 6.1.0 software and average of the data was calculated.

Micro-CT for Colon Wall Thickness

Mice were anesthetized with 1.5–2 % isoflurane, injected with 0.2 ml of 0.4 mg butylscopolamine (Buscopan) i.p., 75 mg Omnipaque (GE Healthcare) i.p., and 0.3 ml $BaSO_4$ rectally. The micro-CT scan started 5 min after injection of the contrast agents. The images were obtained with the Caliper Quantum FX micro-CT system (Perkin Elmer) using a tube voltage of 90 kV, tube current of 160 μA, and a scan time of 4.5 min (field of view $2.4 \times 2.4 \times 2.4$ cm^3, matrix 512^3, $47 \times 47 \times 47$ μm^3). Corresponding to the MRI analysis, colon wall thickness was calculated from reconstructed micro-CT images at three different positions in one axial image position using ImageJ software approximately 1.5 cm proximal to the anus.

PET/CT for Inflammatory Lesions

PET/CT experiments were performed using Inveon multi-modality small animal PET/CT scanner (Siemens Healthcare GmbH, Erlangen, Germany). Mice were anesthetized with 2 % isoflurane and injected with 0.2 ml of 0.4 mg butylscopolamine (Buscopan) i.p., 75 mg Omnipaque (GE Healthcare) i.p., 0.3 ml $BaSO_4$ rectally, and with 30 MBq [^{18}F]FDG i.v. First, a CT scan was acquired; 30 min after i.v. injection of [^{18}F]FDG the PET scan was started. Settings for PET were an acquisition time of 1200 s with a static histogram followed by a FBP (filtered back projection) reconstruction (field of view $10 \times 10 \times 12.6$ cm^3, reconstructed matrix size $128 \times 128 \times 159$, nominal pixel size $0.78 \times 0.78 \times 0.80$ mm^3). Reconstructed images were analyzed using Inveon Research Workplace 3.0 (Siemens Healthcare GmbH). Volumes of interest (VOI) were defined in the distal colon and [^{18}F]FDG uptake was analyzed quantitatively. Mean standardized uptake values were obtained of the VOI. Finally, standardized uptake values (SUVs) were normalized to the injected dose and the body weight of the mice.

Histologic Examination for Colon Wall Thickness and Evaluation of Gut Inflammation

After euthanization, the colons of the mice were removed, fixed in 4 % neutral buffered formalin, embedded in paraffin, cut into 3 μm sections and stained with hematoxylin and eosin. HE stained sections were used for determination of colon wall thickness approximately 1.5 cm from the anus using Zen 2012 blue edition software (Carl Zeiss Microscopy GmbH, Germany). Colon wall thickness was measured at three positions in each axial section.

Blood Examination for Immune Status

Whole blood was collected in EDTA tubes and mixed for 10 min. Afterwards, the samples were measured in ADVIA 120 hematology analyzer (Siemens, Germany).

Statistical Methods

The results are reported as mean ± SD. For body weight and colon wall thickness measurements, comparisons with controls were done by Fisher's LSD test. Colitis and disease activity scores were analyzed by Mann-Whitney test. An α-level of 0.05 was used. Because of the exploratory nature of the study, no adjustments for multiplicity were made.

Results

Administration of 5 Days of DSS-Induced Acute Colitis

For dose finding, 2, 3, or 4 % DSS were added to the drinking water of mice. After 5 days of DSS, mice showed a steady decrease of body weight up to 20 % independent of the DSS dose. At day 8, control mice receiving normal drinking water had a significantly higher body weight with a mean of 22.5 ± 0.9 g compared with 17.4 ± 1.2 g in the 2 % DSS-treated animals ($p < 0.0001$) (Fig. 1a).

DSS application in this model also significantly and dose dependently increased the disease activity index (DAI) reflecting body weight loss, stool consistency, and blood in the stool. In addition to extensive body weight loss, DSS-treated mice suffered from diarrhea and had bloody stools. Consequently, untreated mice had a DAI of 0 over the course of the experiment whereas DSS-treated mice showed a steady increase of the DAI up to 4.72 points in the 4 % DSS group at day 8 (Fig. 1b).

Ex vivo analysis of colons confirmed clinical observations and showed significantly shorter colons due to inflammation and consecutive edema in DSS treated (42.4 ± 6.3 mm for 2 % DSS, 50.5 ± 4.7 mm for 3 % DSS, 46.7 ± 5.6 mm for 4 % DSS) than in control mice (63.3 ± 8.1 mm) ($p < 0.0001$) (Fig. 1c, d).

Endoscopic assessment 8 days (3 and 4 % DSS group) or 9 days (control and 2 % DSS group) after start of the experiment also showed a dose-dependent effect of DSS on changes of the mucosal surface of the mice and could be quantitatively assessed. The mean endoscopic colitis score was significantly higher in DSS-treated animals (5.5 ± 1.3 for 2 % DSS, 6.1 ± 2.1 for 3 % DSS, and 7.3 ± 2.0 for 4 % DSS) compared to control animals (0 over the course of the study) (Fig. 2). Thickening of the colon wall, changed vascular pattern, and fibrin deposits were the most pronounced changes of the mucosa caused by DSS. In contrast, the colon wall of the healthy mice was characterized by a smooth translucent mucosa with normal blood vessel architecture showing no signs of colitis.

DSS Colitis Is Associated with Thickening of the Colon Wall

MRI assessment at day 8 of the study indicated that DSS significantly increased colon wall thickness in colitis mice (Fig. 3a). The mean measured colon wall thickness was significantly higher in DSS-treated mice (0.38 ± 0.05 mm for 2 % DSS, 0.41 ± 0.07 mm for 3 % DSS, and 0.44 ± 0.09 mm
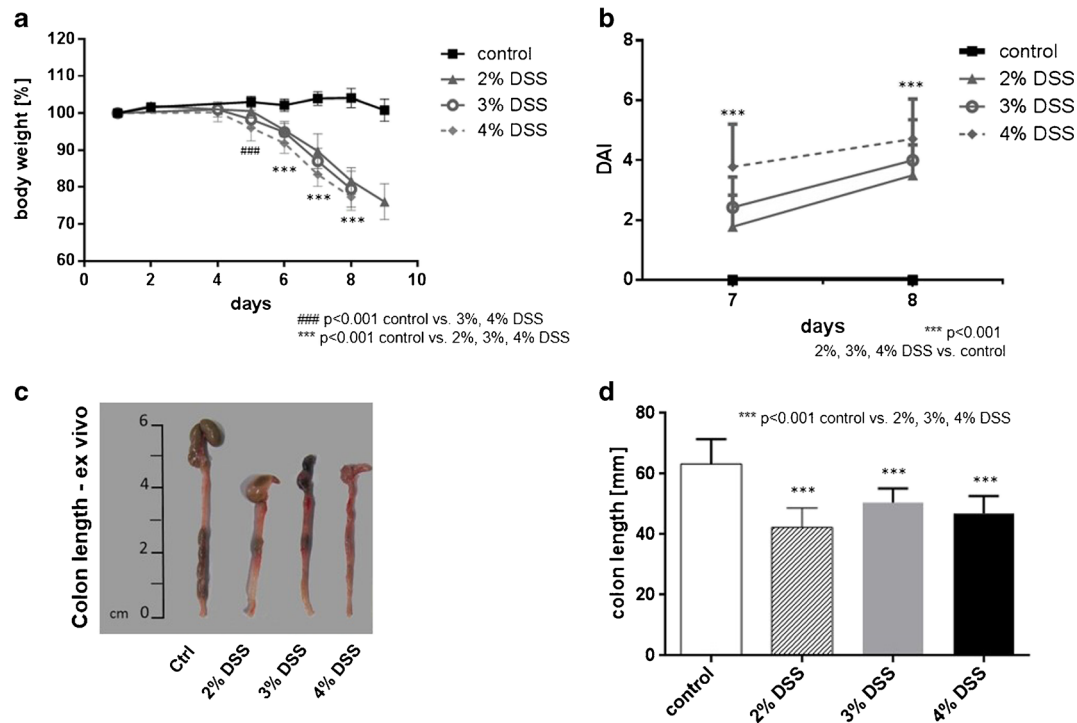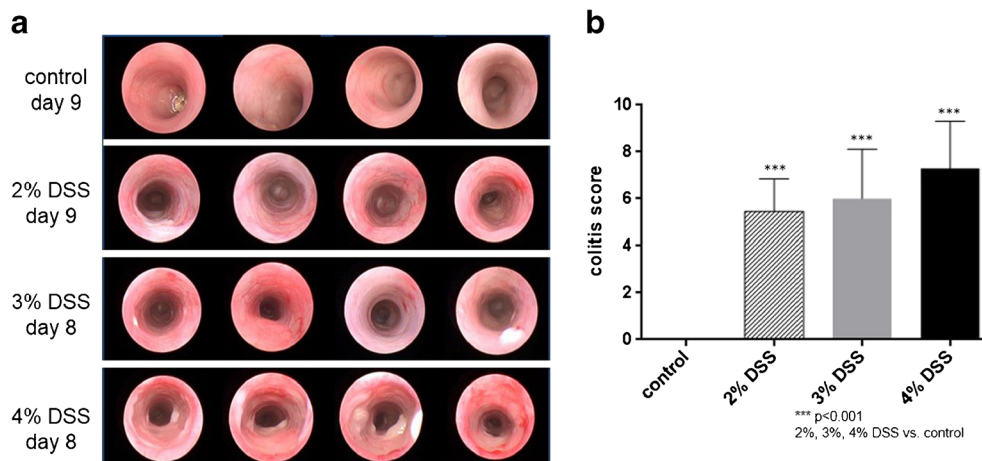
Fig. 1 Administration of 2, 3, or 4 % DSS for 5 days induced acute colitis in mice as assessed by clinical and *ex vivo* observation. **a** Body weight was monitored regularly during the study period. Data are presented as % body weight change from the values at day 0 (control $n = 8$; 2–4 % DSS $n = 14$). **b** The disease activity index (DAI) was assessed at days 7 and 8 (control $n = 8$; 2–4 % DSS $n = 14$). **c** Representative images of colons of control and DSS-treated mice. **d** Length of the colons was significantly shortened in colitis mice (control $n = 6$; 2 % DSS $n = 13$; 3–4 % DSS $n = 14$). Values, mean ± SD.

for 4 % DSS) compared to control animals (0.28 ± 0.04 mm) ($p = 0.0056$; $p = 0.0005$; $p < 0.0001$) (Fig. 3b). There was no statistically significant difference between the different DSS doses.

    The analysis of colon wall thickness as measured by US imaging correlated with the MRI data (Pearson correlation coefficient $r = 0.5118$, $p = 0.0045$; data not shown) showing an increased colon wall thickness in DSS-treated mice although the absolute values of the measurements were different. Quantitation of the colon wall of control animals revealed a thickness of a mean of 0.12 ± 0.06 mm compared to 0.23 ± 0.07 mm, 0.23 ± 0.03 mm, and 0.26 ± 0.04 mm for

Fig. 2 Administration of 2, 3, or 4 % DSS for 5 days induced acute colitis in mice as assessed by colonoscopy. **a** Representative endoscopic images of mucosal changes of control and DSS-treated mice. **b** The murine endoscopic colitis index was assessed at day 9 (control and 2 % DSS) and day 8 (3 and 4 % DSS). Values, mean ± SD; control $n = 8$; 2 % DSS $n = 13$; 3–4 % DSS $n = 14$.
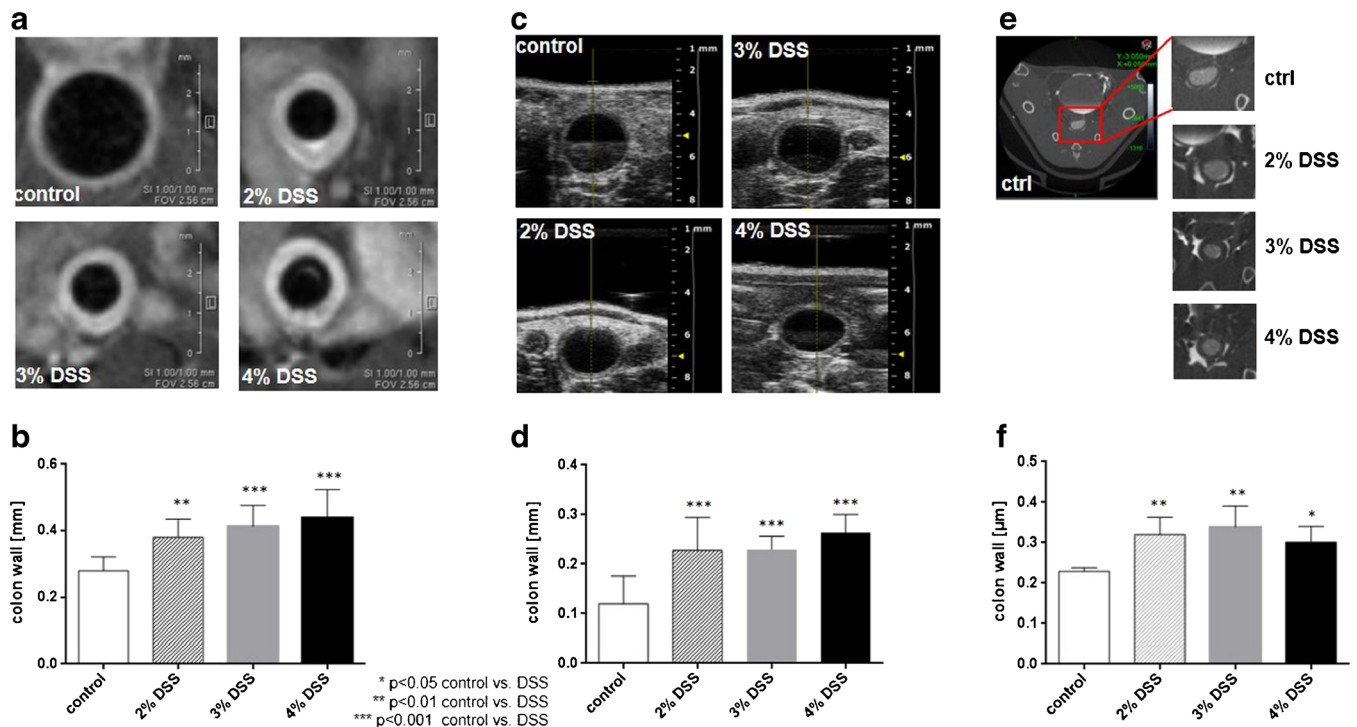
Fig. 3 DSS administration induced an increase of colon wall thickness. **a**, **c**, **e** Representative images of the colon wall of control and DSS-treated animals as measured by **a** MRI, **c** US, and **e** CT. Corresponding quantitation of the colon wall for **b** MRI, **d** US, and **f** CT. Values, mean ± SD; MRI (at day 8): control $n = 6$; 2–4 % DSS $n = 10$; US (at day 8): control $n = 6$; 2 % DSS $n = 9$, 3 % DSS $n = 6$, 4 % DSS $n = 9$; CT (at day 6): control $n = 3$; 2 % DSS $n = 7$, 3 % DSS $n = 7$, 4 % DSS $n = 6$.

2, 3, and 4 % DSS, respectively ($p = 0.0004$; $p = 0.0008$; $p < 0.0001$) (Fig. 3c, d).

In addition to MRI and US, colon wall thickness was determined using CT assessment with both intracolonic (BaSO$_4$) and intraperitoneal (Omnipaque) contrast agent to allow visualization of the colon wall (Fig. 3e). In accordance with the other methods, the CT measurements revealed a higher colon wall thickness in DSS-treated mice with a mean of 0.32 ± 0.04 mm for 2 % DSS, 0.34 ± 0.05 mm for 3 % DSS, and 0.30 ± 0.04 mm for 4 % DSS compared with a mean of 0.23 ± 0.009 mm in healthy control animals ($p = 0.007$; $p = 0.0016$; $p = 0.0287$) (Fig. 3f). A good correlation was evident between both CT and MRI as well as CT and US data (Pearson correlation coefficient $r = 0.6388$ for CT vs. MRI, $p = 0.0139$ and $r = 0.5880$ for CT vs. US, $p = 0.0270$; data not shown).

The accuracy of the imaging data were validated by histological examination of the colons. The colons of control animals showed intact viable mucosa with regularly spaced villi of uniform height whereas in the mucosa of the colons of DSS-treated mice signs of inflammation, crypt damage, and increased colon wall thickness were evident (Fig. 4a). Quantitation of colon wall thickness in multiple sections revealed a significantly higher colon wall thickness in DSS-treated mice (0.39 ± 0.11 for 2 % DSS, 0.43 ± 0.11 mm for 3 % DSS, and 0.42 ± 0.06 mm for 4 % DSS) compared to control animals (0.30 ± 0.06 mm) ($p = 0.0327$; $p = 0.0034$; $p = 0.0053$) (Fig. 4b).

DSS Colitis Is Associated with a High Load of Inflammatory Cells in the Colon Wall

PET/CT measurements at day 7 were used to determine the severity of gut inflammation in colitis mice. The analysis of the data showed an elevated accumulation of [^{18}F]FDG in the inflamed colon walls of DSS-treated animals compared to control animals with the highest uptake in distal parts of the colons indicating an increased degree of gut inflammation in DSS-treated mice (^{18}FDG colon uptake control 0.67 ± 0.20 g/ml; 2 % DSS 1.14 ± 0.36 g/ml; 3 % DSS 1.02 ± 0.35 g/ml; 4 % DSS 1.02 ± 0.37 g/ml) (Fig. 5).

The blood examination revealed an increased number of neutrophils in blood samples of 2 % DSS-treated animals compared to healthy control mice indicating signs of inflammation whereas all other cell types were unchanged compared to the control (data not shown).

Discussion

In this study, we validated and compared correlation of different imaging techniques such as MRI, CT, US, PET/CT as well as colonoscopy to quantify colonic inflammation in the DSS colitis model.

Although colonoscopy is currently the gold standard in routine clinical use [3], its invasiveness and restriction of inspection limited to the mucosal surface make other imaging techniques interesting candidates to overcome these
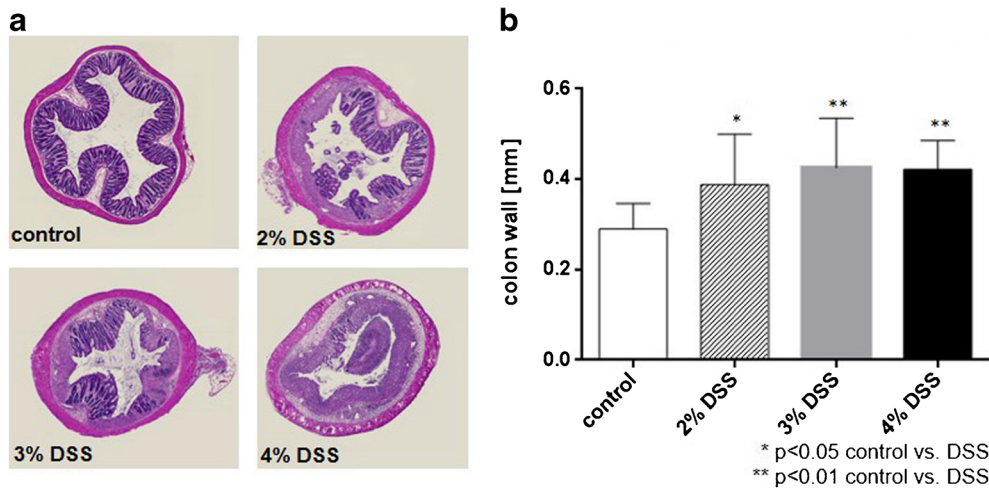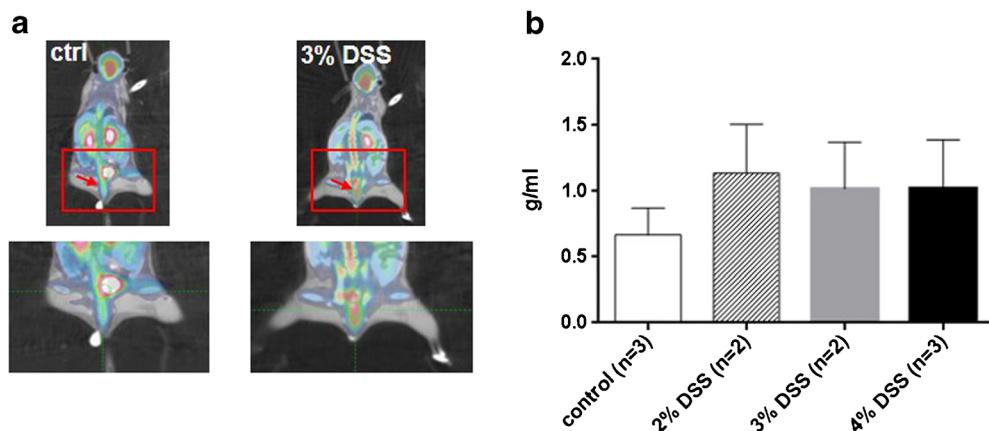
Fig. 4 DSS administration resulted in an increase of colon wall thickness. **a** Representative HE-stained sections of the colon wall of control and DSS-treated animals (control and 2 % DSS at day 9, 3 and 4 % DSS at day 8). **b** Corresponding quantitation of the colon wall thickness assessed from the histologic sections. Values, mean ± SD; control $n = 7$; 2 % DSS $n = 13$; 3 % DSS $n = 14$, 4 % DSS $n = 12$.

limitations. In the present study, MRI, US, and CT were used for anatomical characterization and measurement of the colon wall thickness in the DSS-induced colitis model. Due to its non-invasive character, these techniques were found to be safe, reproducible, and relatively fast. As far as the validation of an imaging readout for colonic inflammation is concerned, all applied imaging methods proved to be feasible for quantitation of the colon wall thickness which was significantly increased after DSS treatment of the mice. The accuracy of the imaging methods was finally validated by histological analysis confirming the increased thickness of the colon wall after DSS administration. Compared to an exclusively histological analysis, a clear advantage of the preclinical use of non-invasive imaging techniques is the need of lower animal numbers as histological examination requires the euthanization of animals at different time points of the study. In line with the 3R concept of animal welfare

[15–17], non-invasive imaging helps to substantially reduce number of animals because animals can be monitored at different points of time and serve as their own control.

Compared to MRI and US, CT assessment requires radiation exposure and the use of contrast agent to properly visualize the colon wall which means additional burden to the animal. Moreover, due to the use of contrast agent, the preparation procedure of the animal was more time consuming compared to MRI and the start of the measurement was time dependent to reach optimal image quality. The considerable time for the measurement could especially be an issue for testing several of compounds allowing no high-throughput screening and scanning of a large number of animals in a manageable time. In this respect, MRI is the preferred imaging method also due to its absence of contrast agent as well as ionizing radiation combined with its high soft-tissue contrast. For the MRI measurement, a soft hollow

Fig. 5 DSS administration resulted in an increased gut inflammation as measured by [18F]FDG-PET/CT imaging. **a** Representative PET/CT images of control and 3 % DSS-treated animals. *Arrows* indicate [18F]FDG uptake in the gut. **b** Corresponding quantitation of the [18F]FDG uptake in the colon of mice. Values, mean ± SD.

tube of small diameter was gently inserted into the distal colon not to damage the mucosa, to avoid folding of the colon and to reach higher, reproducible imaging results. Together with its fast imaging sequence of less than 10 min per animal, MRI would be an ideal method for high-throughput screening in the DSS model. Furthermore, both MRI and CT are cross-sectional methods and visualization of the whole colon in a three-dimensional manner is feasible. As a consequence, they offer the possibility to assess transmural changes of the colon wall as well as fistulas and abscesses which is not regularly possible using, for example, colonoscopy but might be important in a clinical setting. However, transmural or extracolonic changes are no specific characteristics of the DSS model [18] so that the techniques could not be evaluated for this purpose in the study presented. Finally, US imaging was successfully established as a quantitative imaging biomarker in the DSS model. However, the absolute values for colon wall thickness differed between US and MRI. This might be due to the different insufflation methods of the colons of the mice resulting in different degrees of colon expansion. Furthermore, US acquired images of only one slide of the colon without the possibility of allocation to a specific colon segment, and time of the measurement is highly dependent on the skills and experience of the examiner.

Furthermore, PET/CT as functional non-invasive imaging technique was applied in this study as a measure to determine the load of inflammatory cells in the gut. PET/CT is the most time-consuming method applied during this study. Although the animal numbers were low with 2–3 animals per group, a trend to increased PET signal intensity in DSS-treated mice was evident. The signal in the bladder partly obscured the signal in the colon which might be prevented by flushing the bladder during the measurement using a catheter as described by Hindryckx et al. [19]. As also investigated by Hindryckx et al. [19], the increased [18F]FDG uptake in colons might be caused by elevated neutrophil infiltration which is one of the main mediators in DSS-induced colitis [20].

In addition to [18F]FDG PET which is an unspecific tracer of inflammation, it might be more interesting to directly address and track inflammatory cells to better investigate molecular mechanisms of inflammatory bowel disease. As far as nuclear imaging is concerned, several publications describe more specific *in vivo* visualization of the processes of colitis [10]. For example, white blood cell imaging using ^{99m}Tc-hexamethylpropyleneamine oxine ([^{99m}Tc]HMPAO) has been used for diagnosis and therapeutic decision in Crohn's disease [21, 22]. Moreover, IL-2 labeled with Tc-99m, I-123 or F-18 which is released by Th1 (CD4+) lymphocytes showed promising results for the assessment of cell infiltration of activated mononuclear cells in the intestine [23].

But also the aforementioned techniques such as MRI or US allow for specific tracking of different cell types. MRI is described to quantify macrophage activity in the

inflammatory sites using a perfluorocarbon tracer reagent for F-19 MRI [24]. As macrophages also play a role in other diseases of chronic inflammation, this approach could also be used for other inflammatory diseases. In addition, there is no need for radiation for this measurement.

Another example for functional imaging is the use of targeted microbubbles for US imaging which is a widely available, relatively inexpensive technique, and free of radiation. Clinically translatable dual-targeted (P- and E-selectin) microbubbles showed visualization of inflammation within the colon in a murine model of acute colitis [25]. P- and E-selectin have been shown to be expressed on the vasculature during the acute phase of inflammation in IBD patients [26, 27] and are thus useful targets to address.

In addition to diagnostic purposes, the applied imaging modalities—although less frequently used so far compared to conventional colonoscopy—suggest to be also helpful for therapeutic compound screening. As a quantitative readout was established for all methods in this study, all of them could be used to test the efficacy of compounds in the acute DSS colitis model. This hypothesis requires experimental confirmation.

For PET imaging, the feasibility to use [18F]FDG uptake as reliable readout to assess inflammation in the DSS model has been shown by Hindryckx et al. [19]. DMOG treatment known to be effective in DSS-induced colitis [28] resulted in reduced colonic inflammation of colitis mice as detected by decreased [18F]FDG uptake in the colons of treated compared to vehicle animals.

Conclusions

In summary, we showed that the established MRI, US, CT, and PET readouts can be used to reliably assess inflammation in the DSS colitis model with MRI being preferred due to absence of radiation exposure and cross-sectional capacity. The identification of a reproducible model and reliable imaging biomarkers is indispensable to further validate these methods in therapeutic settings, to demonstrate efficacy of IBD targeting compounds, develop new therapies and translate these preclinical results into the clinical setting.

Compliance with Ethical Standards

Conflict of Interest

All the authors are employees of Boehringer Ingelheim Pharma GmbH & Co. K and declare that they have no conflict of interest.

References

1. Podolsky DK (1991) Inflammatory bowel disease (1). N Engl J Med 325:928–937
2. Baumgart DC, Sandborn WJ (2012) Crohn's disease. Lancet 380:1590–1605

3. Hommes DW, van Deventer SJ (2004) Endoscopy in inflammatory bowel diseases. Gastroenterology 126:1561–1573
4. Stange EF, Travis SP, Vermeire S et al (2006) European evidence based consensus on the diagnosis and management of Crohn's disease: definitions and diagnosis. Gut 55(Suppl 1):i1–i15
5. Panes J, Bouhnik Y, Reinisch W et al (2013) Imaging Techniques for assessment of inflammatory bowel disease: joint ECCO and ESGAR evidence-based consensus guidelines. J Crohns Colitis 7:556–585
6. Panes J, Bouzas R, Chaparro M et al (2011) Systematic review: the use of ultrasonography, computed tomography and magnetic resonance imaging for the diagnosis, assessment of activity and abdominal complications of Crohn's disease. Aliment Pharmacol Ther 34:125–145
7. Horsthuis K, Bipat S, Bennink RJ, Stoker J (2008) Inflammatory bowel disease diagnosed with US, MR, scintigraphy, and CT: meta-analysis of prospective studies. Radiology 247:64–79
8. Spier BJ, Perlman SB, Reichelderfer M (2009) FDG-PET in inflammatory bowel disease. Q J Nucl Med Mol Imaging 53:64–71
9. Spier BJ, Perlman SB, Jaskowiak CJ, Reichelderfer M (2010) PET/CT in the evaluation of inflammatory bowel disease: studies in patients before and after treatment. Mol Imaging Biol 12:85–88
10. Glaudemans AW, Maccioni F, Mansi L et al (2010) Imaging of cell trafficking in Crohn's disease. J Cell Physiol 223:562–571
11. Okayasu I, Hatakeyama S, Yamada M et al (1990) A novel method in the induction of reliable experimental acute and chronic ulcerative colitis in mice. Gastroenterology 98:694–702
12. Wirtz S, Neufert C, Weigmann B, Neurath MF (2007) Chemically induced mouse models of intestinal inflammation. Nat Protoc 2:541–546
13. Breynaert C, Dresselaers T, Perrier C et al (2013) Unique gene expression and MR T2 relaxometry patterns define chronic murine dextran sodium sulphate colitis as a model for connective tissue changes in human Crohn's disease. PLoS One 8:e68876
14. Becker C, Fantini MC, Neurath MF (2006) High resolution colonoscopy in live mice. Nat Protoc 1:2900–2904
15. Flecknell P (2002) Replacement, reduction and refinement. ALTEX 19:73–78
16. Rusche B (2003) The 3Rs and animal welfare—conflict or the way forward? ALTEX 20(Suppl 1):63–76
17. Leist M, Kadereit S, Schildknecht S (2008) Food for thought… on the real success of 3R approaches. ALTEX 25:17–32
18. Maxwell JR, Viney JL (2009) Overview of mouse models of inflammatory bowel disease and their use in drug discovery. Curr Protoc Pharmacol 5:Unit 5.57.1–5.58.19
19. Hindryckx P, Staelens S, Devisscher L et al (2011) Longitudinal quantification of inflammation in the murine dextran sodium sulfate-induced colitis model using μPET/CT. Inflamm Bowel Dis 17:2058–2064
20. Dieleman LA, Ridwan BU, Tennyson GS et al (1994) Dextran sulfate sodium-induced colitis occurs in severe combined immunodeficient mice. Gastroenterology 107:1643–1652
21. Arndt JW, Grootscholten MI, van Hogezand RA et al (1997) Inflammatory bowel disease activity assessment using technetium-99m-HMPAO leukocytes. Dig Dis Sci 42:387–393
22. Papós M, Nagy F, Láng J, Csernay L (1993) Technetium-99m hexamethylpropylene amine oxime labelled leucocyte scintigraphy in ulcerative colitis and Crohn's disease. Eur J Nucl Med 20:766–769
23. Signore A, Chianelli M, Annovazzi A et al (2000) 123I-interleukin-2 scintigraphy for in vivo assessment of intestinal mononuclear cell infiltration in Crohn's disease. J Nucl Med 41:242–249
24. Kadayakkara DK, Ranganathan S, Young WB, Ahrens ET (2012) Assaying macrophage activity in a murine model of inflammatory bowel disease using fluorine-19 MRI. Lab Investig 92:636–645
25. Wang H, Machtaler S, Bettinger T et al (2013) Molecular imaging of inflammation in inflammatory bowel disease with a clinically translatable dual-selectin-targeted US contrast agent: comparison with FDG PET/CT in a mouse model. Radiology 267:818–829
26. Schürmann GM, Bishop AE, Facer P et al (1995) Increased expression of cell adhesion molecule P-selectin in active inflammatory bowel disease. Gut 36(3):411–418
27. Jubeli E, Moine L, Vergnaud-Gauduchon J, Barratt G (2012) E-selectin as a target for drug delivery and molecular imaging. J Control Release 158:194–206
28. Cummins EP, Seeballuck F, Keely SJ et al (2008) The hydroxylase inhibitor dimethyloxalylglycine is protective in a murine model of colitis. Gastroenterology 134:156–165